Cohesively Enhanced Conductivity and Adhesion of Flexible Silver Nanowire Networks by Biocompatible Polymer Sol–Gel Transition

*Yunxia Jin, Lu Li, Yuanrong Cheng, Lingqiang Kong, Qibing Pei, and Fei Xiao**

Silver nanowire (AgNW) networks are a promising candidate to replace indium tin oxide (ITO) as transparent conductors. In this paper, a novel transparent composite conductor composed of AgNW/biocompatible alginate gel on a flexible polyethylene terephthalate (PET) substrate, with synchronously enhanced adhesion and reduced resistivity, is prepared without high-temperature annealing. The sheet resistance of the flexible AgNW/PET film reduces from 300 to 50.3 Ohm sq^{-1} at transmittance of 94%. The optical and electrical performance is superior to that obtained from the flexible ITO film on PET. Meanwhile, the sheet resistance does not show great change after tape test, suggesting a good adhesion of AgNW to the polymer substrate. Moreover, the AgNW composite film shows a good stability to resist long-term storage, solvent damage, and ultrasonication. Finally, polymer solar cells employing the composite AgNW film as the electrode are realized, displaying an efficiency of 2.44%.

1. Introduction

Transparent electrodes are widely used in optoelectronics such as liquid crystal displays (LCDs), solar cells, light emitting diodes (LEDs), and many other devices.[1–6] Indium tin oxide (ITO) is commonly used as transparent electrode in many applications but suffers from some crucial drawbacks, such as high cost, scarcity of indium, damage of organic substrates during high-temperature sputtering and lack of flexibility.[7,8] These problems motivate the research for a new transparent conductor, such as single-walled carbon nanotube (CNT) networks, graphene, metal grids, conducting polymers, and random metal nanowire networks.[9–13] Recently, solution-processed silver nanowires (AgNWs) film has become a favored substitute for ITO due to its outstanding mechanical flexibility on flexible substrates and superior opto-electrical performance compared to other competitors.[14–19]

However, several issues need to be addressed for the commercial application of AgNWs film as transparent electrode. First, the strong adhesion between AgNWs and substrate is necessary to resist the detachment. This problem has been improved by modifying the substrate surface, two-step polymer encapsulating, or TiO_2 gel formation.[20–23] Second, the contact resistance across Ag wire–wire junction is considerable due to the capping agent on the surface of AgNW. Thus, a high-temperature thermal annealing at approximately 200 °C is required to improve the conductivity, which restricts the heat-sensitive polymers used as flexible substrates.[24–26] Moreover, AgNW involves a problem of weak stability after high-energy exposure, resulting in the transfer of nanowire to nanoparticles.[16,27] This problem has been improved by importing graphene or graphene oxide to make a hybrid transparent electrode with silver nanowire.[28–30] In sum, most present methods to improve conductivity of AgNW networks rely on high-energy sintering, or enhance the adhesion sacrificing conductivity. The method improving both of the adhesion and conductivity of AgNW film with a good stability via a simple process is very limited.

Recently, a simple sintering agent has been reported to improve the conductivity of metallic nanoparticles (NPs) at room temperature.[31,32] The chloride ions can effectively trigger the coalescence of AgNPs by removing the capping agent on the surface of NPs in a short time. In addition, it is reported that alginate, a salt of alginic acid which is composed of β-D-mannuronic acid (M) and α-L-guluronic acid (G), can be cross-linked by bivalent or polyvalent metal cations to form water-resist gel, which is biocompatible and biodegradable to be used in food and medical industry.[33,34]

Keeping the above introduction in mind, we herein develop a novel sintering method to achieve cohesively enhanced conductive and adhesive AgNW networks on flexible polymer substrate with good stability. In the proposed process, the AgNW networks were deposited on alginate-coated polyethylene terephthalate (PET) substrate by rod coating. Common salt, i.e., $CaCl_2$, was employed as the sintering agent, which not only contained the Cl^- that can detach the anchoring groups of the stabilizer from the surface of AgNW to trigger the sintering,

Y. Jin, Dr. Y. Cheng, L. Kong, Prof. F. Xiao
Department of Materials Science
Fudan University
220 Handan Road, Shanghai 200433, P.R. China
E-mail: feixiao@fudan.edu.cn
Dr. L. Li, Prof. Q. Pei
Department of Materials Sciences and Engineering
California NanoSystems Institute
Henry Samuli School of Engineering and Applied Science
University of California
Los Angeles, CA 90095, USA

DOI: 10.1002/adfm.201403293

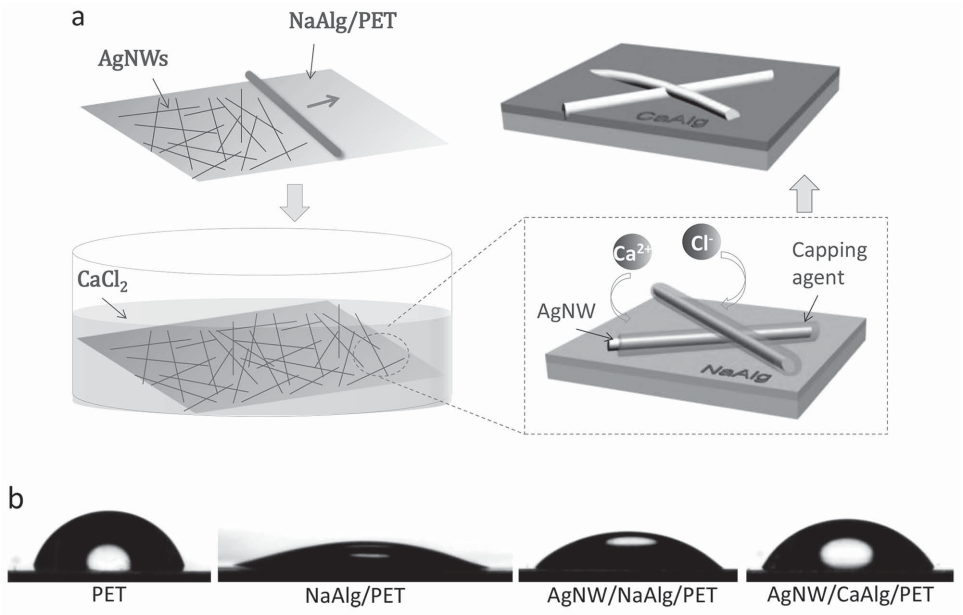

Figure 1. a) A schematic procedure of flexible AgNWs film preparation. b) The hydrophilicity variation during the fabrication process. From left to right the water contact angle is 74.1°, 23.3°, 41.6°, and 61.7°, respectively.

but also possessed bivalent metallic ion Ca^{2+} that can react with the soluble alginate to form water-resist alginate gel to bond the AgNWs tightly on the substrate. This approach can improve the conductivity and adhesion of AgNWs film simultaneously without high-temperature or complicated sintering process. Moreover, the enhanced adhesion in turn improved the conductivity of AgNW film due to the downward force from the adhesive gel to AgNWs. As a result, the fabricated AgNW film showed a sheet resistance reduction from 300 to 53 Ohm sq^{-1}, and an increase of less than 30% after tape test with good solvent-resistance and long-term stability. Moreover, a polymer solar cell employed the prepared AgNW film as bottom electrode was fabricated.

2. Results and Discussion

Figure 1a schematically illustrates the fabrication process of conductive, transparent, and flexible AgNW/gel composite film. Alginate solution was first spin-cast on the clean bare PET substrate. Subsequently, AgNWs dispersion in ethanol was coated onto the prepared NaAlg/PET by a wire-wound rod. At last, AgNW/NaAlg composite electrode was immersed into an aqueous calcium chloride solution for several minutes, followed by washing and drying. By separately depositing adhesive alginate layer and AgNW networks, we eliminated the difficulty of conductivity reduction associated with insulating adhesive locating between crossed AgNWs. The silver nanowire density on the substrate was easily controlled by the AgNW dispersion concentration, the groove space of the wire-wound rod and the rod moving speed. When the AgNW/NaAlg was immersed in calcium chloride aqueous solution, the capping agent surrounded the surface of silver nanowire can be detached by chloride ions, and NaAlg can react with calcium ions to form water-resist CaAlg gel. Therefore, the neighboring crossed Ag nanowires can naturally coalesce together driven by surface tension to achieve a high electrical performance. Besides, the bottoms of AgNWs were buried in the calcium alginate improving the adhesion performance. Meanwhile, the downward force from the calcium alginate to the Ag nanowire enable the deformation of neighboring AgNWs, which further enhanced the electrical connections between crossed AgNWs.

Figure 1b monitors the hydrophilicity variation of the sample during the fabrication process. The water contact angle of bare PET was 74.1°, while it sharply reduced to 23.3° after coating sodium alginate. The significant slide in water contact angle demonstrated the formation of highly hydrophilic layer on the substrate, confirming the deposition of NaAlg. Generally, a hydrophilic surface is helpful for AgNW dispersion to adequately wet the substrate to ensure a relatively more uniform distribution of AgNWs on substrate, while a hydrophobic surface of substrate tends to induce the agglomeration of Ag nanowires to reduce the electrical performance of AgNW film.[25] The contact angle shows an increase to 41.6° after AgNW deposition, and continued to increase to 61.7° after treatment of calcium chloride. The fact of increase of contact angle after calcium chloride treatment is consistent with the prospective progress that alginate sodium react with bivalent metal cation, calcium ion, to produce insoluble polymer alginate calcium gel, which can bond the upper layer of AgNWs to the substrate tightly. Moreover, it is worth noting that alginate is a biocompatible polymer, which benefits the application in bioelectronics.

Figure 2a shows the changes of sheet resistances of pure AgNW networks and AgNW/NaAlg composite depending on the treatment time. The sheet resistances both dropped sharply at the initial stage of treatment, and maintained nearly constant after 10 min. It indicated that the capping agent on the surface of Ag nanowire were detached rapidly as the salt treatment began, improving the connection between crossed AgNWs,

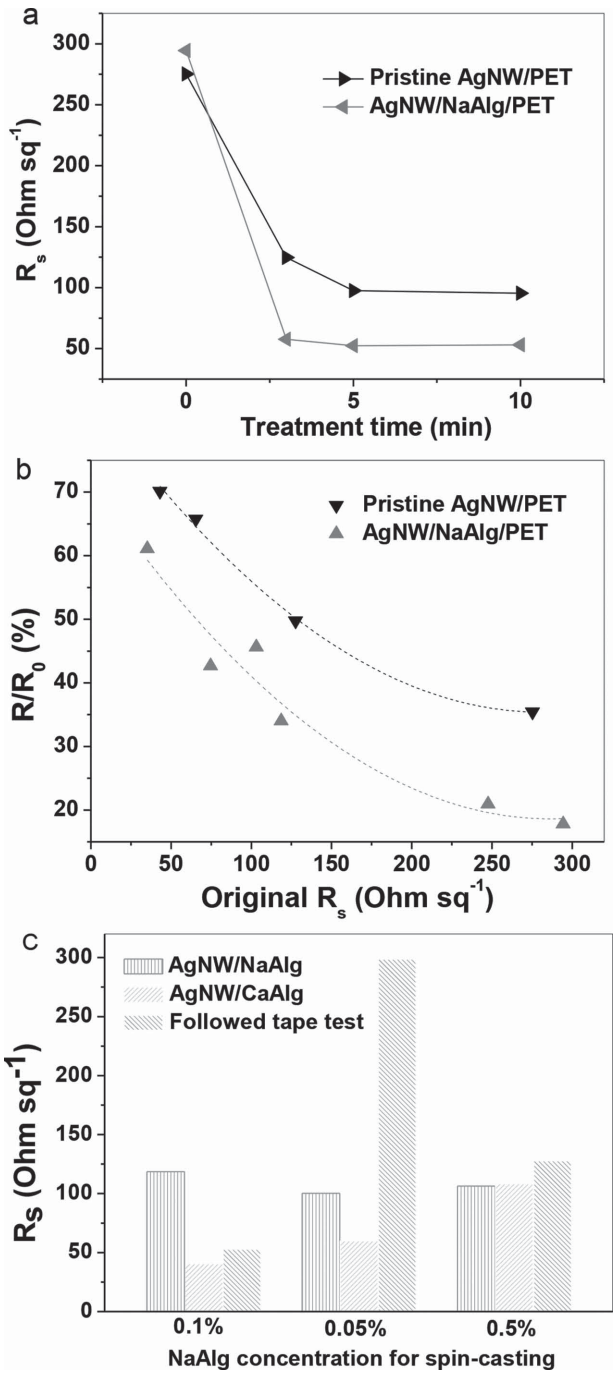

Figure 2. a) Sheet resistance of pristine AgNW film and AgNW/NaAlg composite film depending on immersion time in 5 wt% calcium chloride solution. b) Sheet resistances of pristine AgNW film and AgNW/NaAlg composite film after $CaCl_2$ treatment for 5 min as a function of original value of R_s. c) Sheet resistance changes of AgNW/NaAlg composite film treated by 5 wt% $CaCl_2$ for 5 min (AgNW/CaAlg) and followed tape test depending on different NaAlg thickness.

and hence of the enhanced conductivity. Afterwards, the primary driving force to decrease the contact resistivity transfers to the further coalescence of crossed AgNWs instead of stabilizer detaching. However, this is a much slower process, consequently retarding the reduction trend of resistivity. Therefore, the sheet resistance of AgNW film maintained almost the same at last. But it is obviously shown that the conductivity of AgNW composite film exhibited a deeper decline compared to that of pure AgNW networks after treatment (Figure 2b). The sheet resistance of AgNW/NaAlg composite film dropped by 82% from around 300 to 53 Ohm sq^{-1} after 5 min of treatment of calcium chloride, while it stayed a much larger value of 98 Ohm sq^{-1} for pure AgNWs film. It is noted that the reduction rate of sheet resistance is proportional to the original sheet resistance of AgNW film.

Figure 2c shows the sheet resistance changes of AgNW films after the treatment of calcium chloride and tape test with different adhesive thickness. The standard of test is that the sheet resistance change should be less than 30%, and this requirement varied for different device.[20] With NaAlg concentration of 0.1 wt%, we produced AgNW/CaAlg composite film with sheet resistance decreasing from 118.6 to 40.3 Ohm sq^{-1} after treatment by $CaCl_2$ for 5 min, and only increasing to 52.8 Ohm sq^{-1} after tape test. It suggests the obvious improvement of conductivity and adhesion to substrate of the fabricated AgNWs film. By reducing the NaAlg concentration of spinning solution from 0.1 to 0.05 wt%, the sheet resistance remains almost the same declining trend after $CaCl_2$ treatment. However, this film cannot withstand tape test well, and the sheet resistance moved up sharply to around 5 times. When the concentration was increased to 0.5 wt% the sheet resistance did not show any reduction after $CaCl_2$ treatment, but this film resisted tape test well of which the sheet resistance only changed from 108.3 to 127.8 Ohm sq^{-1}. It is noted that the sol-gel transition of alginate is fast which can be done within several minutes. So when the AgNW was embedded in massive alginate the chloride ions would not get enough time to trigger the sintering before the AgNWs were fixed in their original positions by CaAlg. Moreover, some single AgNWs may be already separated from each other by the massive surrounding CaAlg, which disabled the sintering of AgNW. In a word, the results here indicated that the adhesive gel rendered the conductivity and adhesion of AgNW networks on PET, but preferred thickness of adhesive was necessary to get both good conductivity and adhesion.

By optimizing the process conditions with 0.1 wt% of NaAlg solution for spinning cast and 5 min of treatment of 5 wt% $CaCl_2$ aqueous solution, we produced highly opto-electrical AgNW/CaAlg composite film on PET. **Figure 3**a shows the transmittances of the AgNW/CaAlg composite films and ITO on PET. The transmittances of AgNW composites were nearly constant over the visible light, while the transmittance for ITO film was sharply reduced near the UV region and exhibited fluctuations over the region of visible light. The AgNW/CaAlg composite film showed a sheet resistance of 30.6 Ohm sq^{-1} for 92.5% transmittance at 550 nm. Generally, higher transmittance means less AgNWs on the substrate, resulting in higher sheet resistance. Thus, the performances of the transparent conductive films were compared using the ratio of DC to optical conductivity (σ_{DC}/σ_{Op}) defined by Equation (1)

$$T(\lambda) = \left(1 + \frac{188.5}{R_s}\frac{\sigma_{Op}(\lambda)}{\sigma_{DC}}\right)^{-2} \quad (1)$$

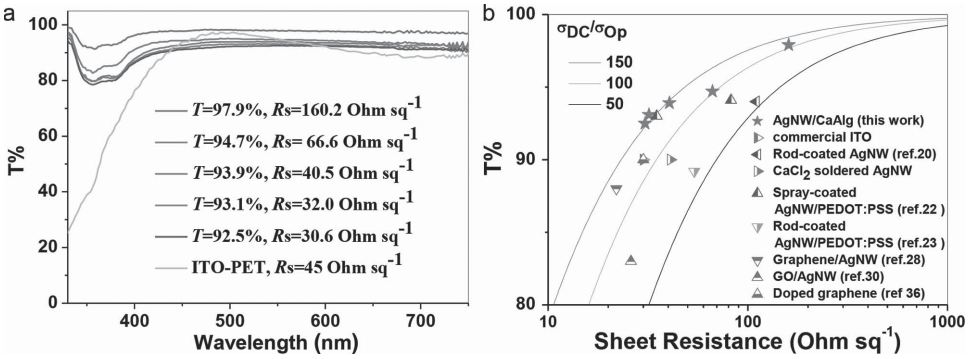

Figure 3. a) The optical transmittance spectra of AgNW/CaAlg composite network and ITO on PET substrate. b) Plot of optical transmittance versus sheet resistance. The literature reported values are also shown for comparison.

where $\sigma_{Op}(\lambda)$ is the optical conductivity, σ_{DC} is the DC conductivity, T is the transmittance, and R_s is the sheet resistance of the film.[14] This expression was first employed by Hu et al. to estimate the opto-electrical performance of CNT, and matched with the experimental data well.[35] Then it was widely used for different kinds of transparent electrodes. Here it was fitted to the data in Figure 3b using three different values of σ_{DC}/σ_{Op} = 150, 100, and 50 (solid lines). It is desired to maintain a high value of σ_{DC}/σ_{Op} for transparent conductive film, which corresponds to low surface resistivity and high optical transmission. Generally, the value of σ_{DC}/σ_{Op} drops down with transmittance increasing. However, all the experimental values here at high transmittance still located in the range of σ_{DC}/σ_{Op} = 100–160. The best σ_{DC}/σ_{Op} value of AgNW electrode is up to 350 obtained by vacuum filtration or rod-casting of AgNW/clay mixture.[14] However, it reduced to 50–85 when adhesion of AgNW to substrate was improved. Recently, the highest values of σ_{DC}/σ_{Op} in the range of 70–150 at high transmittance (93%–94%) could be obtained from the AgNW composite film with doped conducting polymer PEDOT:PSS.[22] Our AgNW/CaAlg composite film revealed a σ_{DC}/σ_{Op} value of 154 at 92.5% transmittance, which is higher than that of commercial ITO on PET (σ_{DC}/σ_{Op} = 100–150), graphene and hybrid electrode of silver nanowire.[28,30,36]

The scanning electron microscopy (SEM) images of AgNW film after treatment and tape test were used to determine the reason of both improvement of conductivity and adhesion. **Figure 4** shows the changes of silver nanowires triggered by the post-treatment of chloride ions and calcium ions. Initially, each AgNW was lightly laid on the neighboring nanowires or substrate with limited point contact or line contact (Figure 4a). Sharp images with clear shine sides are always observed at crossed AgNWs position of pristine AgNW networks. This phenomenon, however, drastically declined or even disappeared when AgNW networks were treated with calcium chloride (Figure 4b). In Figure 4c, AgNW/CaAlg composite film not only showed the declined or disappeared shine edges as that observed in Figure 4b, but also exhibited obvious shape deformation of upper Ag nanowires along with the lower Ag nanowires. This is due to the downward force exerted by the alginate gel between substrate and AgNW networks. Thus, the electrical contact between crossed AgNWs will be further enhanced, which is consistent with the results revealed in Figure 2b.

Figure 5a,b shows the photographs of AgNW networks on PET before and after tape test. The pristine AgNW network is known to be easily detached from the substrate by tape. A clear boundary near the dashed red line in Figure 5a can be observed after tape test. Moreover, few silver nanowires were left on the

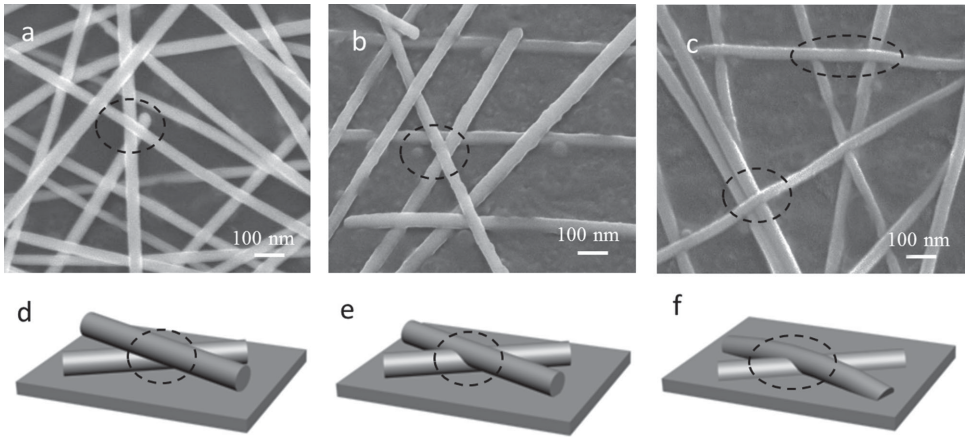

Figure 4. SEM images of a) pristine AgNWs film; b) pristine AgNW film treated by 5 wt% calcium chloride aqueous solution for 5 min. c) AgNW/CaAlg composite film. d,e,f) Schematic diagrams of AgNWs on PET corresponding to (a,b,c).

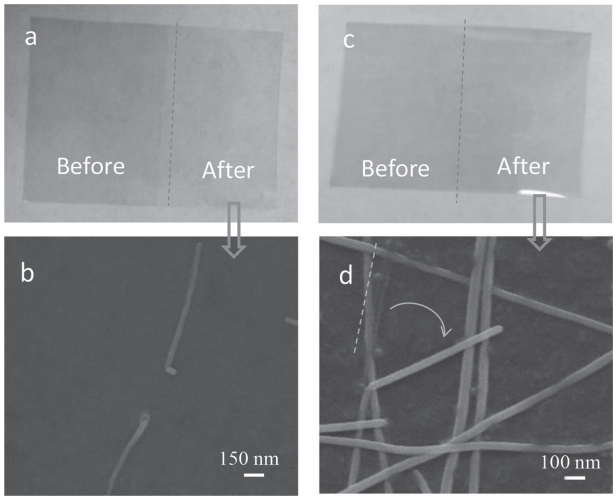

Figure 5. Photographs before and after tape test and the SEM images after tape test of a,b) pristine AgNW film and c,d) AgNW/CaAlg composite film.

PET (Figure 5b). However, there is no obvious visual change for the AgNW/CaAlg composite film after tape test, demonstrating significantly increased adhesion of AgNW to the substrate (Figure 5c). Besides, most Ag nanowires of AgNW/CaAlg composite film stayed in the original positions and kept their shapes on the substrate after tape test as shown in Figure 5d. A part of one single nanowire was observed detached from the substrate, but still stayed on the substrate due to the strong adhesion of the other part of the same nanowire. A clear scallop near the dashed green line was left, which was supposed to be the original position of the detached part of the nanowire. It suggests that the bottom parts of Ag nanowires were partially embedded in the layer of alginate calcium, but the upper parts are still exposed to air or in contact with other nanowires. This is the crucial reason for the high conductivity and strong adhesion of Ag nanowire to substrate simultaneously.

The stability of AgNW film is a critical requirement to ensure the practical application. It has been reported that the morphology of AgNW changed a lot after high-energy sintering, of which nanoparticles or knurls can be observed within several hours.[27] The similar change was also detected in pristine AgNW after treatment by chloride ions at room temperature, as shown in **Figure 6**a. Nanoparticles on the surface of Ag nanowire were observed in the SEM image during the early storage in air. At last the whole Ag nanowires were fully corroded to lose their initial shape, and only vary-shaped particles were left. These suggest that the large amount of chloride residue and high-energy exposure are not preferred for the long-term stability of AgNWs. The morphology of our AgNW/CaAlg composite film obtained from low-temperature process was shown in Figure 6b, it revealed almost no change after 40 days. It means the water flushing, enabled by the enhanced adhesion of AgNW to the substrate, removed the chloride ions sufficiently. However, more research is needed to investigate the long-term stability of AgNW with trace of chloride ions, since the chloride is also the main impurity during the synthesis of AgNW. For practical application of AgNW, the electrode also needs to resist the chemical damage. Thus the electrode can

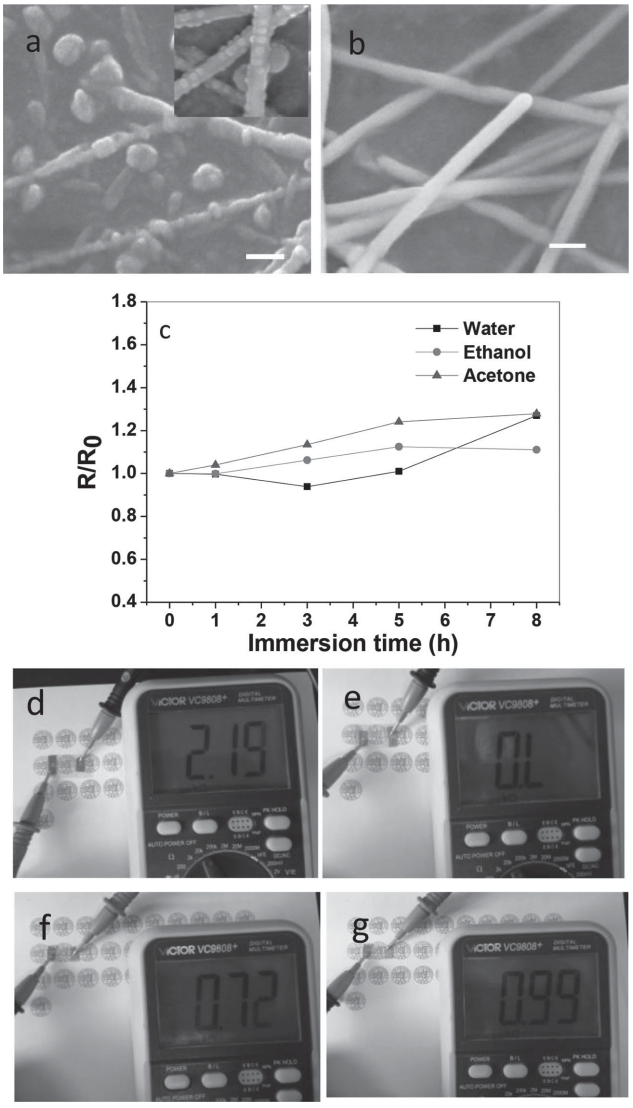

Figure 6. SEM images of $CaCl_2$ treated a) pristine AgNW cleaned by immersion in water, and b) AgNW/CaAlg composite film flushed by water stored in ambient environment for 40 days. Inset is the SEM image of a) in the early stage. The scale bar is 100 nm. c) Sheet resistance change of AgNW/CaAlg composite film depending on immersion time in water, ethanol, and acetone. d–g) Resistance of AgNW/PET (d,e) and AgNW/CaAlg/PET (f,g) before and after ultrasonication in water with 300 W of power and 40 kHz of frequency for 10 s.

survive during the solution-process of the device manufacturing and not influence the long-term stability of the device. The standard of these tests is also reported that the sheet resistance changed by less than 30%.[20] Figure 6c shows that the sheet resistance change by less than 30% after immersion in water, ethanol, and acetone for 8 h. Moreover, the fabricated AgNW composite film still maintained its conductivity even being ultrasonicated for 10 s, while the pristine AgNW becomes an insulator when experiences the same treatment. It suggests the good stability exposure to common solvent.

Flexibility is an essential requirement for transparent electrode used in the flexible devices. However, ITO is too fragile to be used as a flexible electrode. AgNWs film is a good candidate

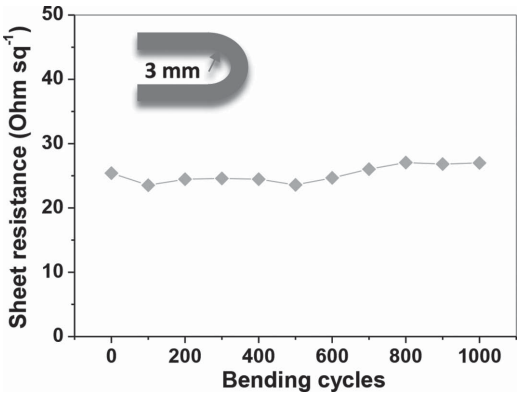

Figure 7. Sheet resistances of AgNW/CaAlg composite film as a function of bending cycles. The bending radius is 3 mm.

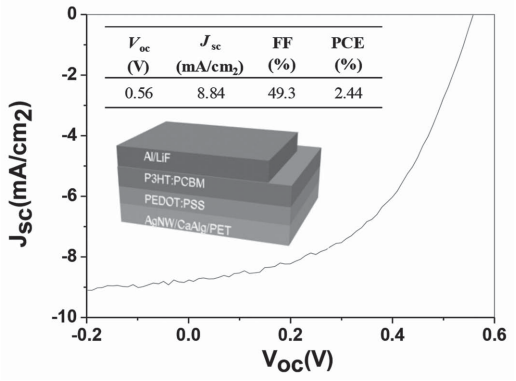

Figure 8. Current density versus voltage, schematic drawing, and key parameters for the device based on AgNW/CaAlg composite as the bottom electrode.

to replace the ITO, but the high-temperature thermal-annealing sintering process disabled AgNWs depositing on the low-cost flexible polymer substrate with low thermal stability. Here due to the low-temperature process of the proposed fabrication of AgNW/CaAlg composite film, flexible transparent conductive film on low-cost PET was prepared. As shown in **Figure 7**, 1000 cycles of bending test was conducted with a bending radius of 3 mm to explore the flexibility of strongly adhesive AgNW film on PET substrate. The sheet resistance of AgNW composite film was maintained nearly at a constant value during the cyclic bending test. It is notable that the AgNW/CaAlg composite film exhibits a good tolerance to bending. Combined with the results of adhesion and electrical performance, it suggests that AgNW film with good conductivity, strong adhesion, and good flexibility was successfully fabricated on a PET substrate via the proposed simple and fast sol-gel transition technique, which is important for high-performance flexible devices.

Finally, polymer solar cell was fabricated as described in the Experimental Section. The prepared AgNW/CaAlg film on PET was employed as the bottom electrode. Poly(3,4-ethyl enedioxythiophene):poly(styrenesulfonate) (PEDOT:PSS) was used as the buffer layer, and blend of poly(3-hexylthiophene) (P3HT) and phenyl-C61-butyric acid methyl ester (PCBM) with 1:1 weight ratio as the active layer. Al/LiF was deposited on the top as the cathode. The photovoltaic performance was presented in **Figure 8**. The device showed a short circuit current of 8.84 mA cm^{-2}, an open circuit voltage of 0.56 V and fill factor of 49.3%, resulting in a relatively high power conversion efficiency (PCE) of 2.44%. The reported PCE of P3HT solar cell is 1.8% based on ITO/PET,[37] and 3.2% on ITO/glass.[38]

3. Conclusions

We developed a simple method to demonstrate cohesively enhanced adhesion and conductivity of AgNW on low-cost polymer flexible substrate without high-temperature annealing. On one hand, the bivalent calcium ions in calcium chloride cross-linked the alginate under the AgNW networks to form water-resist alginate gel to bond the AgNWs tightly on the substrate. On the other hand, the chloride ions in calcium chloride detached the anchoring groups of the stabilizer on the surface of Ag nanowire to trigger the sintering. The adhesion enhancement of AgNW to substrate in turn improved the conductivity due to the downward force exerted by the adhesive gel on AgNWs. This process removed the high-temperature annealing to make it applicable for various heat-sensitive polymer as the substrate of transparent electrode. As a result, flexible and stable AgNW film with sheet resistance of 32 Ohm sq^{-1} and transmittance of 93.1% was obtained, and does not show great change after tape test, long-term storage, and solvent immersion. A P3HT polymer solar cell is realized with PCE of 2.44%. We expect that this work is helpful for development of high-performance flexible transparent electrode for flexible electronics.

4. Experimental Section

Preparation of AgNWs Film: Sodium alginate (Aladdin Reagent Corp.) was dissolved in water to form a uniform solution (0.1 wt%), and then spinning-coated on a clean PET substrate (3000 rpm, 60 s), marked as NaAlg/PET. The AgNWs (40 nm in diameter and 15 μm in length) dispersion in ethanol (Blue Nano) was diluted to a concentration of 1 mg mL^{-1}, and rod coated on the alginate modified PET, marked as AgNW/NaAlg/PET. The as-prepared film was then treated by calcium chloride aqueous solution with concentration of 5 wt% for several minutes. At last, the AgNWs film was rinsed by water and dried at 80 °C for 30 min, labeled as AgNW/CaAlg/PET.

Polymer Solar Cell Fabrication: AgNW/CaAlg/PET with a sheet resistance of 22 Ohm sq^{-1} and transmission of 90% at 550 nm was put successively in deionized water, acetone, and isopropyl alcohol for 10 min for cleaning. Filtrated PEDOT:PSS aqueous solution (AI4083 from H. C. Stark) was preheated at 90 °C for 30 min and then spin-cast on AgNW film at 4000 rpm for 60 s. The PEDOT:PSS was then annealed at 130 °C for 20 min. The active layer was coated following literature procedures:[39] poly(3-hexylthiophene) (P3HT) and phenyl-C61-butyric acid methyl ester (PCBM) were mixed with 1:1 weight ratio and co-dissolved in 1,2-dichlorobenzen with final P3HT concentration of 20 mg mL^{-1}. The resulting solution was spin-cast at 600 rpm for 60 s. The solvent was dried out after about 20 min in a covered glass petri-dish. The active layer was further thermally annealed at 140 °C for 5 min, resulting in a 210 nm thick blend layer. A 1 nm thick LiF layer and a 100 nm thick aluminum were then consecutively deposited by physical vapor deposition at 3×10^{-6} mbar to complete the device fabrication. The active device area defined by the shadow mask for the cathode deposition was 14 mm^2.

Characterization: The water contact angle was determined by an OCA15 contact angle analyzer (Dataphysics, Germany) using a 5 μL deionized water droplet. Optical transmission spectra of AgNW films were taken with a T6 new century spectrophotometer (PGeneral, China) with a clean bare PET substrate as a reference. The sheet resistances were measured using a 4-point probe system (SB100A/2), and obtained from the averaged values of several positions on one sample. The adhesive test was done as follows: A 12 mm-wide 3M scotch tape was attached to the sample, and then slowly peeled off from the sample. Scanning electron microscopy (SEM) micrographs were taken on a 6701F field emission scanning electron microscope (FE-SEM, JEOL). Current density–voltage (*J–V*) characteristics were measured with a Keithley 2400 Semiconductor Characterization System. The photovoltaic performance was measured under an air mass of a 1.5 solar illumination at 100 mW cm^{-2} (1 sun).

Acknowledgements

Y.J. and L.L. contributed equally to this work. This study was supported by National Science and Technology Major Project with Contract No. 2013ZX02505.

Received: September 21, 2014
Revised: November 19, 2014
Published online: January 29, 2015

[1] D. S. Hecht, L. Hu, G. Irvin, *Adv. Mater.* **2011**, *23*, 1482.
[2] L. Hu, H. Wu, Y. Cui, *MRS Bull.* **2011**, *36*, 760.
[3] L. Li, Z. Yu, W. Hu, C. H. Chang, Q. Chen, Q. Pei, *Adv. Mater.* **2011**, *23*, 5563.
[4] J. Zhang, Y. Fu, C. Wang, P. C. Chen, Z. Liu, W. Wei, C. Wu, M. E. Thompson, C. Zhou, *Nano Lett.* **2011**, *11*, 4852.
[5] S. Seobálee, S. Hwanáko, *Nanoscale* **2012**, *4*, 6408.
[6] M. Song, D. S. You, K. Lim, S. Park, S. Jung, C. S. Kim, D. H. Kim, D. G. Kim, J. K. Kim, J. Park, Y. C. Kang, J. Heo, S. H. Jin, J. H. Park, J. W. Kang, *Adv. Funct. Mater.* **2013**, *23*, 4177.
[7] R. B. H. Tahar, T. Ban, Y. Ohya, Y. Takahashi, *J. Appl. Phys.* **1998**, *83*, 2631.
[8] D. R. Cairns, R. P. Witte Ii, D. K. Sparacin, S. M. Sachsman, D. C. Paine, G. P. Crawford, R. Newton, *Appl. Phys. Lett.* **2000**, *76*, 1425.
[9] M. W. Rowell, M. D. Mcgehee, *Energy Environ. Sci.* **2011**, *4*, 131.
[10] K. H. Lee, S. M. Kim, H. Jeong, Y. Pak, H. Song, J. Park, K. H. Lim, J. H. Kim, Y. S. Kim, H. C. Ko, I. K. Kwon, G. Y. Jung, *Adv. Mater.* **2013**, *25*, 3209.
[11] D. M. Sun, C. Liu, W. C. Ren, H. M. Cheng, *Small* **2013**, *9*, 1188.
[12] Y. Jin, Y. Cheng, D. Deng, C. Jiang, T. Qi, D. Yang, F. Xiao, *ACS Appl. Mater. Inter.* **2014**, *6*, 1447.
[13] J. Liang, L. Li, K. Tong, Z. Ren, W. Hu, X. Niu, Y. Chen, Q. Pei, *ACS Nano* **2014**, *8*, 1590.
[14] S. De, T. M. Higgins, P. E. Lyons, E. M. Doherty, P. N. Nirmalraj, W. J. Blau, J. J. Boland, J. N. Coleman, *ACS Nano* **2009**, *3*, 1767.
[15] E. C. Garnett, W. Cai, J. J. Cha, F. Mahmood, S. T. Connor, M. Greyson Christoforo, Y. Cui, M. D. McGehee, M. L. Brongersma, *Nat. Mater.* **2012**, *11*, 241.
[16] J. Jiu, M. Nogi, T. Sugahara, T. Tokuno, T. Araki, N. Komoda, K. Suganuma, H. Uchida, K. Shinozaki, *J. Mater. Chem.* **2012**, *22*, 23561.
[17] T. Kim, Y. W. Kim, H. S. Lee, H. Kim, W. S. Yang, K. S. Suh, *Adv. Funct. Mater.* **2013**, *23*, 1250.
[18] J. Lee, I. Lee, T.-S. Kim, J.-Y. Lee, *Small* **2013**, *9*, 2887.
[19] Y. Jin, D. Deng, Y. Cheng, L. Kong, F. Xiao, *Nanoscale* **2014**, *6*, 4812.
[20] L. Hu, H. S. Kim, J. Y. Lee, P. Peumans, Y. Cui, *ACS Nano* **2010**, *4*, 2955.
[21] R. Zhu, C. H. Chung, K. C. Cha, W. Yang, Y. B. Zheng, H. Zhou, T. B. Song, C. C. Chen, P. S. Weiss, G. Li, Y. Yang, *ACS Nano* **2011**, *5*, 9877.
[22] D. Y. Choi, H. W. Kang, H. J. Sung, S. S. Kim, *Nanoscale* **2013**, *5*, 977.
[23] J. Lee, P. Lee, H. B. Lee, S. Hong, I. Lee, J. Yeo, S. S. Lee, T.-S. Kim, D. Lee, S. H. Ko, *Adv. Funct. Mater.* **2013**, *23*, 4171.
[24] J. Y. Lee, S. T. Connor, Y. Cui, P. Peumans, *Nano Lett.* **2008**, *8*, 689.
[25] A. Madaria, A. Kumar, F. Ishikawa, C. Zhou, *Nano Res.* **2010**, *3*, 564.
[26] W. Gaynor, G. F. Burkhard, M. D. Mcgehee, P. Peumans, *Adv. Mater.* **2011**, *23*, 2905.
[27] H. G. Im, J. Jin, J. H. Ko, J. Lee, J. Y. Lee, B. S. Bae, *Nanoscale* **2014**, *6*, 711.
[28] R. Chen, S. R. Das, C. Jeong, M. R. Khan, D. B. Janes, M. A. Alam, *Adv. Funct. Mater.* **2013**, *23*, 5150.
[29] S. Xu, B. Man, S. Jiang, M. Liu, C. Yang, C. Chen, C. Zhang, *Cryst. Eng. Comm.* **2014**, *16*, 3532.
[30] I. N. Kholmanov, M. D. Stoller, J. Edgeworth, W. H. Lee, H. Li, J. Lee, C. Barnhart, J. R. Potts, R. Piner, D. Akinwande, J. E. Barrick, R. S. Ruoff, *ACS Nano* **2012**, *6*, 5157.
[31] M. Grouchko, A. Kamyshny, C. F. Mihailescu, D. F. Anghel, S. Magdassi, *ACS Nano* **2011**, *5*, 3354.
[32] Y. Tang, W. He, G. Zhou, S. Wang, X. Yang, Z. Tao, J. Zhou, *Nanotechnology* **2012**, *23*, 355304.
[33] J. W. Rhim, J. H. Lee, S. I. Hong, *LWT – Food Sci. Tech.* **2006**, *39*, 806.
[34] S. Zhou, A. Bismarck, J. H. G. Steink, *J. Mater. Chem. B* **2013**, *1*, 4736.
[35] L. Hu, D. S. Hecht, G. Grüner, *Nano Lett.* **2004**, *4*, 2513.
[36] S. Bae, H. Kim, Y. Lee, X. Xu, J.-S. Park, Y. Zheng, J. Balakrishnan, T. Lei, H. R. Kim, Y. I. Song, *Nat. Nanotechnol.* **2010**, *5*, 574.
[37] O. Ourida, B. M. Said, T. Thierry, S. B. Martin, *J. Energy Power Eng.* **2014**, *8*, 107.
[38] Z. Yu, L. Li, Q. Zhang, W. Hu, Q. Pei, *Adv. Mater.* **2011**, *23*, 4453.
[39] G. Li, V. Shrotriya, J. Huang, Y. Yao, T. Moriarty, K. Emery, Y. Yang, *Nat. Mater.* **2005**, *4*, 864.